Inorganic Chemistry

Article

pubs.acs.org/IC

Lead(II) Binding to the Chelating Agent D-Penicillamine in Aqueous Solution

Natalie S. Sisombath, Farideh Jalilehvand,* Adam C. Schell, and Qiao Wu

Department of Chemistry, University of Calgary, 2500 University Drive NW, Calgary, Alberta T2N 1N4, Canada

Supporting Information

ABSTRACT: A spectroscopic investigation of the complexes formed between the Pb(II) ion and D-penicillamine (H_2Pen), a chelating agent used in the treatment of lead poisoning, was carried out on two sets of alkaline aqueous solutions with $C_{Pb(II)}$ ≈ 10 and 100 mM, varying the H_2Pen/Pb(II) molar ratio (2.0, 3.0, 4.0, 10.0). Ultraviolet−visible (UV-vis) spectra of the 10 mM Pb(II) solutions consistently showed an absorption peak at 298 nm for $S^- \rightarrow$ Pb(II) ligand-to-metal charge-transfer. The downfield ^{13}C NMR chemical shift for the penicillamine COO^- group confirmed Pb(II) coordination. The ^{207}Pb NMR chemical shifts were confined to a narrow range between 1806 ppm and 1873 ppm for all Pb(II)-penicillamine solutions, indicating only small variations in the speciation, even in large penicillamine excess. Those chemical shifts are considerably deshielded, relative to the solid-state ^{207}Pb NMR isotropic chemical shift of 909 ppm obtained for crystalline penicillaminatolead(II) with Pb(*S,N,O*-Pen) coordination. The Pb L_{III}-edge extended X-ray absorption fine structure (EXAFS) spectra obtained for these solutions were well-modeled with two Pb−S and two Pb-(N/O) bonds with mean distances 2.64 ± 0.04 Å and 2.45 ± 0.04 Å, respectively. The combined spectroscopic results, reporting $\delta(^{207}Pb) \approx 1870$ ppm and $\lambda_{max} \approx 298$ nm for a $Pb^{II}S_2NO$ site, are consistent with a dominating 1:2 lead(II):penicillamine complex with $[Pb(S,N,O\text{-Pen})(S\text{-}H_n\text{Pen})]^{2-n}$ (n = 0−1) coordination in alkaline solutions, and provide useful structural information on how penicillamine can function as an antidote against lead toxicity *in vivo*.

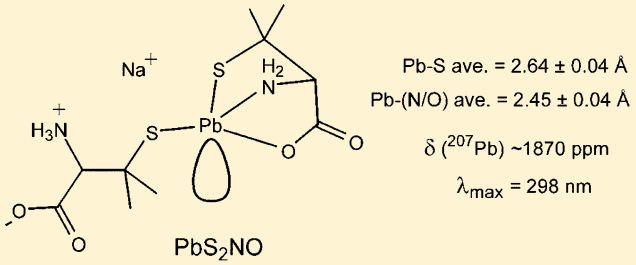

INTRODUCTION

Environmental and occupational sources continue to make lead exposure a health hazard, despite the restrictions to use lead in gasoline and paints over the past few decades. The largest current industrial use of lead is in production of lead-acid batteries for automobiles.[1,2] Lead persists in drinking water, old paint, dust, soil, ceramics, and some toys and food.[3,4] Recently, cocoa used in manufacturing chocolate has been identified as a significant source of lead ingestion.[5] The use of lead solder and leaded pipes in public water supply systems has been banned in many countries; however, leaded plumbing components still contribute to lead exposure. Dust and soil contaminated from the deterioration of old paint are the primary sources of lead exposure to children.[6] Harmful biological effects even occur at low blood lead level (BLL) concentrations, especially in children. Permanent developmental and behavioral problems in children associated with lead poisoning occur at lower BLL concentrations than adults and most symptoms experienced by adults can be treated.[7]

The bioaccumulation pattern of lead(II) in selected organs of *Catla Catla* fingerlings has been identified as kidney > liver > gill > brain > muscle.[8] Divalent lead is known to affect the function of at least three major organ systems, including the central nervous system, the heme biosynthetic pathway, and the renal system.[9−11] Lead(II) frequently targets Ca(II) and Zn(II) binding proteins, displacing the essential metal ions and altering the geometry of active site environments, thus inhibiting substrate binding and catalysis of key metalloenzymes.[7,12] δ-Aminolevulinic acid dehydratase (ALAD) is an example of an enzyme that can be inhibited by lead. ALAD is a catalyst in the heme biosynthetic pathway and contains a zinc-binding site, where the Zn(II) ion is attached to three cysteine residues in tetrahedral coordination geometry. Lead(II) binds more tightly to this site than zinc(II), forming trigonal pyramidal coordination geometry with the three cysteinyl groups. As a result, lead(II), at high BLLs, can deactivate this enzyme and cause anemia.[13−15] To remove lead, chelating agents that form strong bonds to heavy metals can be utilized.

Chelation therapy has been largely used for lead(II) detoxification since the early 1950s.[16−19] Calcium disodium EDTA ($CaNa_2$EDTA), dimercaprol (BAL), D-penicillamine, and 2,3-dimercaptosuccinic acid (DMSA or succimer) have been used as clinical chelating agents for Pb(II), with D-penicillamine being the only orally administered drug available until succimer in 1991.[20,21] In the United States, succimer and $CaNa_2$EDTA are the first and second choices as chelating agents for lead poisoning. D-penicillamine is a third-line drug in the United States, while it is listed as the alternative to succimer in the United Kingdom.[22] Theoretical calculations show that Pb(II) ions can displace Fe(II), Zn(II), Cu(II), or Zn(II) ions bound to BAL or D-penicillamine, but it can only replace Ca(II)

Received: August 5, 2014
Published: November 11, 2014

bound to EDTA, i.e., the latter is a less-selective chelating agent *in vivo*, binding more favorably to Cu(II) and Zn(II) ions.[23] In fact, zinc depletion has been observed when using $EDTA^{4-}$.[24] Research also shows that a limited dose of D-penicillamine is effective in treating children with mild to medium levels of lead poisoning, while showing some transient adverse effects (e.g., rash, decrease in white blood cells count).[25] Succimer is still the drug of choice for oral chelation therapy of lead-poisoned patients, because of the increased side effects of D-penicillamine when used in higher doses.[26]

Penicillamine (H_2Pen) has three potential coordinating sites that after deprotonation can bind to the Pb(II) ion. The acid dissociation constants of penicillamine in aqueous solution are pK_{a_1} = 1.81, pK_{a_2} = 7.96, and pK_{a_3} = 10.72. The carboxyl group deprotonates first to carboxylate (COO^-) in a zwitterion (see Scheme 1), in which the amino (NH_3^+) and thiol (SH) groups

Scheme 1. Zwitterionic Form of Penicillamine (H_2Pen)

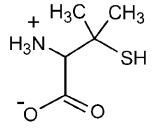

H_2Pen

deprotonate almost simultaneously to form thiolate (S^-) and amine (NH_2) binding sites.[27] Kuchinskas and Rosen reported formation constants for 1:1 and 1:2 complexes between Pb(II) and penicillamine in aqueous solution, assuming bidentate (*S,N*) coordination (C_{H_2Pen} = 3.33 mM, $H_2Pen/Pb(NO_3)_2$ molar ratio = 2:0, pH = 3.5−10.3, 0.15 M KNO_3, 25 °C).[28] However, Lenz and Martell interpreted the potentiometric titration curve differently, considering formation only of a 1:1 complex between Pb(II) and a tridentate (*S,N,O*) penicillamine in aqueous solution (C_{H_2Pen} = 3.0 mM, $H_2Pen/Pb(II)$ molar ratio = 2.0, pH = 2−11, 0.10 M KNO_3, 25 °C).[29] Later, Corrie et al. reported formation constants for several Pb(II)-penicillamine complexes in aqueous solution: PbPen, $[Pb(HPen)]^+$, $Pb(HPen)_2$, $[Pb(Pen)(HPen)]^-$, $[Pb(Pen)_2]^{2-}$, and $[Pb(Pen)_2(OH)]^{3-}$ ($H_2Pen/Pb(II)$ molar ratios = 1.0−8.0, I = 3.0 M $NaClO_4$, 25 °C); see Figure S-1a in the Supporting Information.[30] More recently, Crea and co-workers also reported a new set of formation constants based on potentiometric measurements for PbPen, $[Pb(HPen)]^+$, $[Pb(H_2Pen)]^{2+}$, $[Pb(Pen)_2]^{2-}$, and $[Pb(Pen)(OH)]^-$ ($0.5 \leq C_{H_2Pen} \leq 2.0$ mM, $C_{Pb(II)}$ = 0.5 mM, pH = 2.5−10.5, $0 < I \leq 1.0$ M $NaNO_3$, 25 °C); see Figure S-2a in the Supporting Information.[31] At such low concentrations, no PbPen(c) precipitation was observed, and there is no solubility product/formation constant reported for this solid.

In the crystalline PbPen compound, penicillamine acts as a tridentate ligand in a 1:1 complex with Pb(II) (see Scheme 2). The same 1:1 compound crystallizes over a wide pH range from ∼2 to ∼11, even at high ligand:metal ratios.[32,33] The stability of this compound is probably due to the weak interactions between neighboring complexes in the PbPen crystal.[32] No attempt has been made previously to structurally characterize the Pb(II) complexes with penicillamine in solution.

The purpose of the current study is to gain better insight on how Pb(II) ions are bound by the chelating agent D-penicillamine in aqueous solution, characterizing the coordination and complexes formed by a combination of different spectroscopic techniques, including ^{207}Pb NMR, ^1H NMR, and ^{13}C NMR, extended X-ray absorption fine structure (EXAFS) spectroscopy, and electron-spray ionization mass spectrometry (ESI-MS).

Scheme 2. Polymeric Structure of PbPen[33]

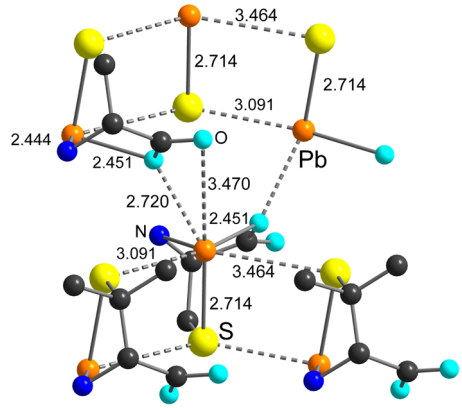

EXPERIMENTAL SECTION

Sample Preparation. D-Penicillamine, $Pb(ClO_4)\cdot 3H_2O$, and sodium hydroxide were used as supplied from Sigma−Aldrich. Two sets of solutions with $C_{Pb(II)}$ = 10 and 100 mM, respectively, were prepared with different $H_2Pen/Pb(ClO_4)_2$ molar ratios (2.0, 3.0, 4.0, and 10.0; Table 1) at the alkaline pH at which the initially formed

Table 1. Composition of Pb(II)-Penicillamine Solutions

$H_2Pen/Pb(II)$ molar ratio	pH	solution	$C_{Pb(II)}$ (mM)	solution	$C_{Pb(II)}$ (mM)
2.0	10.3 (A), 11.0 (A*)	A	10	A*	100
3.0	9.6	B	10	B*	100
4.0	9.6	C	10	C*	100
10.0	9.6	D	10	D*	100

PbPen microcrystals dissolve. To measure the ^{207}Pb NMR spectra of solutions containing $C_{Pb(II)}$ = 10 mM, enriched ^{207}PbO (94.5%) obtained from Cambridge Isotope Laboratories was dissolved in 0.1 M $HClO_4$. All preparations were performed in an argon atmosphere using deoxygenated water, prepared by bubbling argon gas through boiled deionized water. The pH of the aqueous solutions was monitored with a Thermo Scientific Orion Star pH meter calibrated with standard buffers.

The Pb(II)-penicillamine solutions A−D (see Table 1) were freshly prepared before measurements by adding $Pb(ClO_4)_2\cdot 3H_2O$ (0.05 mmol) to dissolved H_2Pen (0.1−0.5 mmol) in deoxygenated water. Upon dropwise addition of sodium hydroxide (1.0 M), a white precipitate was formed (pH 2.4). Sodium hydroxide was added until the precipitate dissolved, giving a clear colorless solution above pH 9. For solutions A and A* ($H_2Pen/Pb(II)$ molar ratio = 2.0), the pH had to be increased to 10.3 and 11.0, respectively, to completely dissolve the solid. The final volume for each solution was set to 5.0 mL. These solutions (A−D) were used for ^1H and ^{13}C NMR (prepared in 99.9% deoxygenated D_2O), ESI-MS, and UV-vis measurements. The pH-meter reading for solutions prepared in D_2O was 10.3 for solution A (pD = pH reading + 0.4),[34] and 9.6 for solutions B−D. Solutions A*−D* containing $C_{Pb(II)}$ = 100 mM were prepared in a similar way. Pb L_{III}-edge EXAFS and ^{207}Pb NMR (10% v/v D_2O) spectra were measured for all solutions. Crystalline PbPen was prepared for ^{207}Pb solid-state NMR measurements by mixing 9.0 mmol $Pb(ClO_4)_2\cdot 3H_2O$ with 15.0 mmol penicillamine in 17 mL of O_2-free water under an

dx.doi.org/10.1021/ic5018714 | Inorg. Chem. 2014, 53, 12459−12468

argon atmosphere. The precipitate was filtered, washed with water, dried under vacuum, and identified by CHN elemental analyses and unit-cell dimensions.[32,33]

Mass Spectrometry (MS). Electrospray ionization mass spectrometry (ESI-MS) spectra were collected both in positive (+) and negative (−) ion modes on an Agilent 6520 Q-Tof instrument by direct infusion of solutions A and D, using water as the mobile phase. The capillary voltage was set at 4 kV, the skimmer voltage was set at 65 V, and the fragmentor voltage was set at 120.0 V. A continuous injection flow rate of 0.2 mL min^{-1} and a drying gas flow rate of 7 L min^{-1} at 200 °C were used.

NMR Spectroscopy. All NMR measurements were carried out at room temperature (~300 K). ^{207}Pb NMR spectra for solutions A−D enriched in ^{207}Pb were collected using a Bruker AMX 300 spectrometer equipped with a 10 mm broad-band probe at resonance frequency of 62.93 MHz. A Bruker Avance 400 MHz spectrometer with a 5 mm broad-band probe was used to measure ^{207}Pb NMR spectra for solutions A*−D* at a resonance frequency of 83.68 MHz. The ^{207}Pb chemical shift for solutions was externally calibrated relative to 1.0 M $Pb(NO_3)_2$ solution in D_2O, resonating at −2961.2 ppm, relative to $Pb(CH_3)_4$ (δ = 0 ppm).[35] The ^{207}Pb NMR data were acquired using a 30° pulse, a 66.7 kHz sweep width, a 1.0-s delay time between scans, and 16K data points. Approximately 12 000−51 000 scans were co-added. Spectra were processed using exponential line broadening (10% of the line width at half-maximum).

Cross-polarization magic angle spinning (CP/MAS) ^{207}Pb NMR spectra for the PbPen solid were measured with high power proton decoupling on a Bruker Avance III 200 NMR spectrometer at room temperature [(^{207}Pb) 41.94 MHz]. The ground solid was packed into a 7-mm zirconia rotor, spinning at MAS rates of 5.8 and 5.5 kHz, collecting 15360 and 4290 scans, respectively, with a 2.0-s recycle delay. The proton 90° pulse was 3.75 μs; a 10 ms contact time was used for cross-polarization with a ramped X pulse. Chemical shifts were referenced relative to $Pb(CH_3)_4$, by setting the ^{207}Pb NMR peak of solid $Pb(NO_3)_2$ spinning at 1.7 kHz rate at −3507.6 ppm (295.8 K).[36,37] Static ^{207}Pb NMR powder patterns were reconstructed by iteratively fitting the sideband manifold using the Solids Analysis package within Bruker's TOPSPIN 3.2 software.

^{13}C and ^{1}H NMR spectra of solutions A−D were measured using a Bruker Avance II 400 MHz spectrometer at a resonance frequency of 100.64 and 400.18 MHz, respectively. ^{13}C NMR spectra were collected using a 30° pulse, a 26.2 kHz sweep width, a 1-s delay between scans, and 32K data points. A total of 900−5000 scans were co-added, and the spectra were externally calibrated using CH_3OH in D_2O, resonating at 49.15 ppm. ^{1}H NMR spectra were collected using a 30° pulse, a 6.4 kHz sweep width, 32K data points, and a 0.5-s delay between scans. Between 16 and 32 scans were co-added, and the spectra were internally referenced using the HOD/H_2O peak at 4.80 ppm.

Electronic Spectroscopy. UV-vis absorption spectra for solutions A−D were measured at room temperature, using a Cary 300 UV-vis double-beam spectrophotometer. Samples were measured in quartz cells with a path length of 1 mm, using a 1.5 absorbance Agilent rear-beam attenuator (RBA) mesh filter in the reference position.

EXAFS Data Collection. Pb L_{III}-edge X-ray absorption spectra for solutions A*, C*, and D* were collected at BL 2−3 (100 mA), and for solutions A−D and B* at BL 7−3 (500 mA) at the Stanford Synchrotron Radiation Lightsource (SSRL) operating under 3 GeV. Higher-order harmonics were rejected by detuning a Si(220) (ϕ = 0°) double-crystal monochromator to 50% of maximum I_0 intensity at the end of the Pb L_{III}-edge scan range at BL 2−3, and by using a Rh-coated harmonic rejection mirror positioned after a Si(220) (ϕ = 90°) double-crystal monochromator at BL 7−3. The latter crystals showed several glitches in I_0 at high k. Therefore, the XAS spectra for solutions A−D and B* were noisier than those of solutions A*, C*, and D* measured at BL 2−3 equipped with Si(220) ϕ = 0° monochromator crystals. To avoid photoreduction of the samples at BL 7−3, the beam size was set to 1 mm × 1 mm and the intensity of the incident beam was detuned to 80% of maximum I_0 at 13 806 eV. The X-ray energy was internally calibrated by placing a Pb foil between the I_1 and I_2 ion chambers, and assigning the first inflection point in its absorption spectrum to 13 035.0 eV. Solutions were held between 5 μm polypropylene windows in 5 mm Teflon sample holders, placed between ion chambers I_0 and I_1. All ion chambers were filled with nitrogen gas (N_2). XAS spectra of solutions A*−D* were measured in transmission mode, collecting three scans for each sample. For the dilute solutions A−D, 10−20 scans were collected in both transmission and fluorescence modes simultaneously, measuring Pb L_α X-ray fluorescence radiation emitted from the sample using a 30-element germanium solid-state detector array. All detector channels for each scan were examined to check the quality of the data. All individual scans were compared prior to averaging, to ensure that no radiation damage occurred during measurement. However, even after removing poor quality data from several Ge-detector channels in the data averaging process, still the averaged transmission data were less noisy than the fluorescence data. Therefore, for all Pb(II)-penicillamine solutions, the XAS data obtained in transmission mode were further processed.

EXAFS Data Analysis. EXAFS oscillations were extracted using the WinXAS 3.1 program,[38] subtracting the background in the pre-edge region using a first-order polynomial, followed by normalization of the edge step. The threshold energy (E_0) varied over a narrow range of 13034.3−13034.8 eV, and was used for converting energy unit to k space (Å^{-1}), where $k = [(8\pi^2 m_e/h^2)(E - E_0)]^{1/2}$. The structural parameters were extracted following the procedure explained earlier.[39] The crystal structure of D-penicillaminatolead(II)[33] (PbPen) was used in the ATOMS program, creating the input file for the FEFF 7.0 program.[40,41] For each backscattering path, the structural parameters that were refined in the least-squares curve-fitting procedure included the bond distance (R), the Debye−Waller parameter (σ^2), and sometimes the coordination number (N), keeping the amplitude reduction factor (S_0^2) fixed at 0.9 (as obtained from EXAFS curve-fitting for solid PbPen),[39] allowing ΔE_0 (a common value for all paths) to float.

RESULTS

ESI-Mass Spectrometry. To identify possible Pb(II)-penicillamine complexes formed in solution, ESI-MS spectra of solutions A and D, containing $C_{Pb(II)}$ = 10 mM with different H_2Pen/Pb(II) molar ratios (2.0 and 10.0, respectively), were measured both in positive- and negative-ion mode by direct infusion of these solutions in the instrument.

The spectra in positive ion mode (see Figure 1, as well as Figure S-3 in the Supporting Information) or negative ion mode (see Figure S-4 in the Supporting Information) display similar peaks with somewhat different intensities; the peak assignments are described in Table 2, as well as Table S-1 in the Supporting Information. The isotopic distribution of naturally occurring lead facilitates the assignment of Pb(II)-containing ions in the ESI-MS spectra via the characteristic pattern: ^{208}Pb (52.4%), ^{207}Pb (22.1%), and ^{206}Pb (24.1%). In positive-ion mode, peaks associated with Pb(II)-containing mass ions $Pb(HPen)^+$ (m/z = 356.02 atomic mass units (amu)), $Pb(Pen)Na^+$ (378.00 amu), $Pb(H_2Pen)(HPen)^+$ (505.07 amu), and $(Pb(Pen))_2Na^+$ (733.01 amu) were observed, some of which may have formed in the gas-phase due to protonation, fragmentation or adduct formation (see Table 2). In the negative-ion mode, only a singly charged lead(II) complex ion $Pb(Pen)(HPen)^-$ is observed at m/z 503.05 amu (see Figure S-4 in the Supporting Information).

Electronic Absorption Spectroscopy. The UV-vis spectra for solutions A−D show an intense peak in the far-UV region (~255 nm) and a less-intense peak at ca. 298 nm (Figure 2), both of which have been assigned as a combination of ligand-to-metal charge transfer (LMCT) (S^- 3p → Pb^{II} 6p) and Pb(II) intra-atomic transitions (e.g., Pb^{II} 6s → 6p).[42−45]

dx.doi.org/10.1021/ic5018714 | Inorg. Chem. 2014, 53, 12459−12468

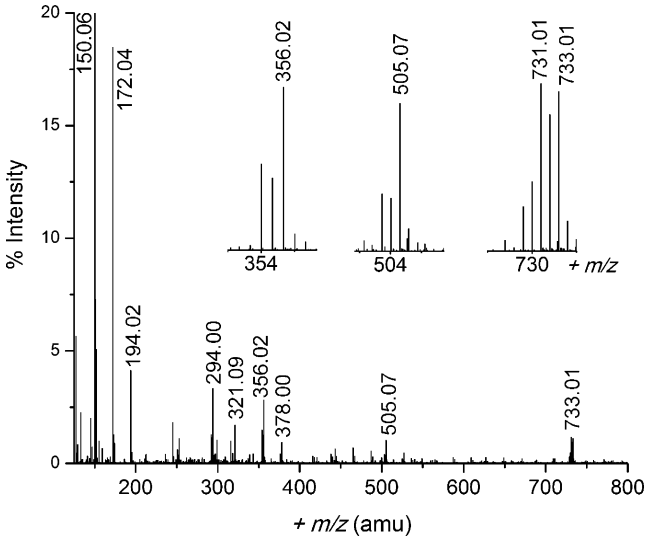

Figure 1. ESI-MS spectrum measured in the positive-ion mode for solution A (H_2Pen/Pb(II) molar ratio = 2.0, $C_{Pb(II)}$ = 10 mM, pH 10.3); the peak at 150.06 amu has 100% relative intensity.

Table 2. Assignment of Mass Ions Observed in ESI-MS Spectra (Positive (+) Mode) for Pb(II)-Penicillamine Solutions A and D ($C_{Pb(II)}$ = 10 mM, H_2Pen/Pb(II) Molar Ratio of 2.0 and 10.0, Respectively)[a]

m/z (amu)	assignment	*m/z* (amu)	assignment
150.06	$[H_2Pen + H^+]^+$	356.02	$[Pb(H_2Pen) - H^+]^+$
172.04	$[Na^+ + H_2Pen]^+$	378.00	$[Na^+ + Pb(H_2Pen) - 2H^+]^+$
194.02	$[2Na^+ + H_2Pen - H^+]^+$	505.07	$[Pb(H_2Pen)_2 - H^+]^+$
294.00	$[2Na^+ + H_2Pen + ClO_4^-]^+$	514.11	$[3Na^+ + 3(H_2Pen) - 2H^+]^+$
321.09	$[Na^+ + 2(H_2Pen)]^+$	536.09	$[4Na^+ + 3(H_2Pen) - 3H^+]^+$
343.07	$[2Na^+ + 2(H_2Pen) - H^+]^+$	733.01	$[Na^+ + Pb_2(H_2Pen)_2 - 4H^+]^+$

[a] H_2Pen ($C_5H_{11}NO_2S$); m = 149.05.

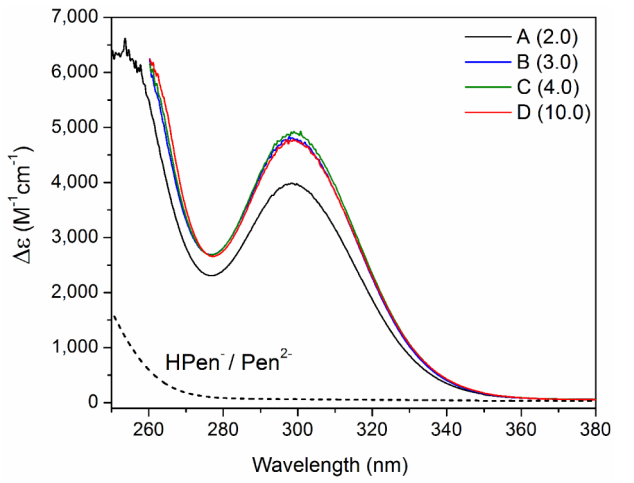

Figure 2. UV-vis spectra of alkaline aqueous Pb(II)-penicillamine solutions A–D containing $C_{Pb(II)}$ = 10 mM and H_2Pen/Pb(II) molar ratios of 2.0–10.0, compared with that of free penicillamine (10 mM, pH 9.6).

For solution A with a H_2Pen/Pb(II) molar ratio of 2.0 (pH 10.3), the amplitude of the peak at 298 nm is ~17% lower.

^{1}H- and ^{13}C NMR Spectroscopy. Figure 3 displays ^{1}H and ^{13}C NMR spectra for a 0.1 M penicillamine solution (pH 9.6) and the Pb(II)-penicillamine solutions A–D ($C_{Pb(II)}$ = 10 mM), all prepared in D_2O. Because of the fast ligand exchange on the NMR time scale, an average signal is observed for both coordinated and free penicillamine in the Pb(II)-containing solutions (solutions A–D). ^{13}C NMR signals show a downfield shift for the carbon sites C_1, C_2, and C_3, relative to free penicillamine; see Table S-2 in the Supporting Information. Similarly, ^{1}H NMR peaks for H_a and methyl H_c protons in free penicillamine became deshielded in the Pb(II)-containing solutions (solutions A–D).

^{207}Pb NMR Spectroscopy. ^{207}Pb is an attractive nucleus for NMR studies: it has a natural abundance of 22.1%, $I = {}^1/_2$ nuclear spin and a receptivity of 11.7, relative to ^{13}C. Its chemical shift spans over a wide range (~17 000 ppm) and is sensitive to changes in the local structure, coordination number, and electronic environment around the ^{207}Pb nucleus, concentration, and temperature.[35,36,46–48] The nature of the bonding (covalent versus ionic) between the Pb(II) ion and the donor atom of the ligand and its polarizability influences the shielding around the Pb nucleus; for biologically relevant donor atoms the shielding increases in the order S < N < O.[35,46,49]

Despite the great interest in Pb(II) thiolate interactions in biological environments, there are only a limited number of reports on ^{207}Pb NMR chemical shifts for Pb(II)-thiolate coordination, including $PbSN_2$ (2357 ppm),[50] solid-state PbS_2N (δ_{iso} = 2852 ppm), PbS_2N_2 (δ_{iso} = 2105–2733 ppm) and PbS_2NS' (δ_{iso} = 2873 ppm; S′ = bridging thiolate),[51,52] PbS_2O_2 (1506–1555 ppm),[53] PbS_3 in peptides (2577–2853 ppm),[39,54] and PbS_3O_3 (1422–1463 ppm).[55] Note that the different electron-donating ability of a particular donor atom (e.g., N in pyridine versus amine) can affect the electronic environment around the ^{207}Pb nucleus, and influence the ^{207}Pb NMR chemical shift. This has been observed in the isotropic ^{207}Pb NMR chemical shifts for two PbS_2N_2 complexes (2,6-$Me_2C_6H_3S)_2Pb(py)_2$ and $Pb(S_2CH_2CH_2NH_2)$ with δ_{iso} = 2733 and 2105 ppm, respectively.[51,52]

Here, we report the solid-state ^{207}Pb NMR isotropic chemical shift for the PbPen complex, together with ^{207}Pb NMR spectra for Pb(II)-penicillamine alkaline aqueous solutions.

Crystalline PbPen has a polymeric structure, where the Pb(II) ion is surrounded by a tridentate (*S,N,O*)-Pen^{2-} ligand; the thiolate S/carboxylate O atoms form bridges between neighboring Pb(II) ions, creating a distorted pentagonal coordination bipyramidal geometry $PbSNOS'_2O'_2$ (S′, O′ = bridging groups). There is a void between the two S′ atoms in the equatorial plane (see Scheme 2),[33] for an antibonding MO state, traditionally ascribed to a stereochemically active inert electron pair (see ref 39 and refs therein). Figure 4, as well as Figure S-5a in the Supporting Information, show the CP/MAS ^{207}Pb NMR spectra of crystalline PbPen measured at two different spin rates (5.5 and 5.8 kHz). By reconstructing the static powder pattern for the spin rate 5.8 kHz, the following principal components were obtained: δ_{11} = 2221.05 ppm; δ_{22} = 1762.88 ppm; δ_{33} = −1255.6 ppm, resulting in $\delta_{iso} = {}^1/_3(\delta_{11} + \delta_{22} + \delta_{33})$ = 909.4 ppm (see Figure S-5b in the Supporting Information). This isotropic chemical shift is considerably upfield, relative to the reported chemical shifts for PbS_3O_3 coordination.[55] Earlier reports suggest that an increase in the

dx.doi.org/10.1021/ic5018714 | Inorg. Chem. 2014, 53, 12459–12468

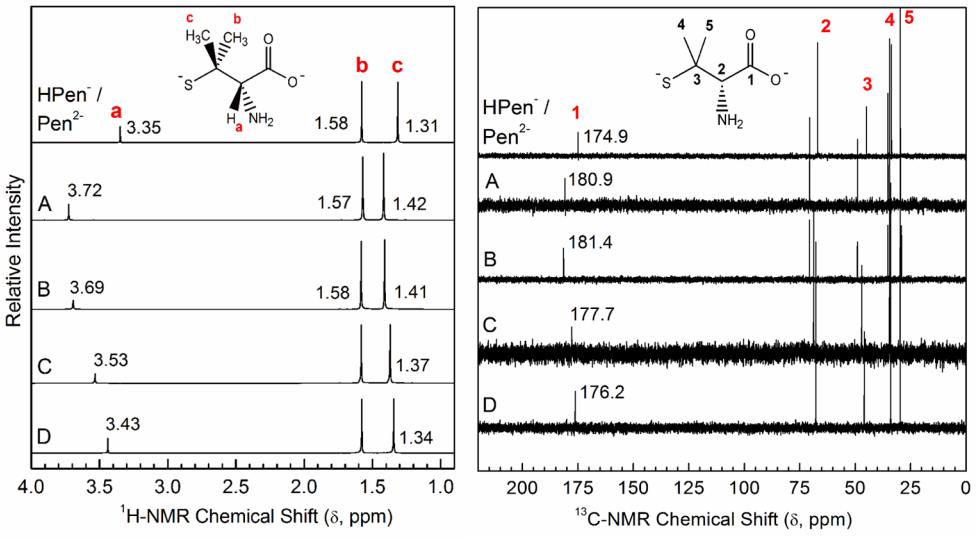

Figure 3. ^{1}H- and ^{13}C NMR spectra of 0.1 M penicillamine in D_2O (pH 9.6) and Pb(II)-penicillamine alkaline solutions (99.9% D_2O) containing $C_{Pb(II)}$ = 10 mM and with H_2Pen/Pb(II) molar ratios of (A) 2.0, (B) 3.0, (C) 4.0, and (D) 10.0; see Table 1.

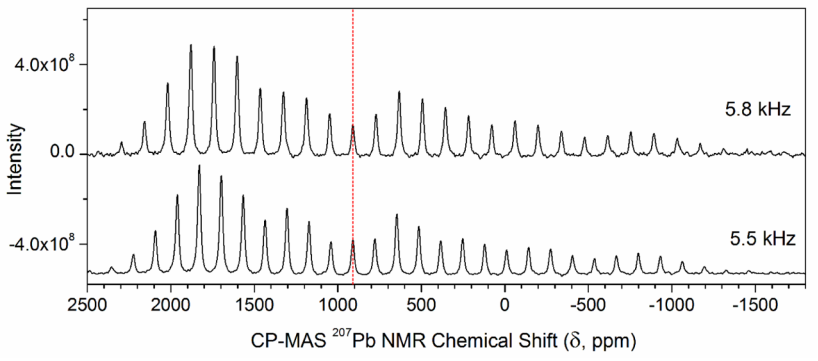

Figure 4. Cross-polarization magic angle spinning (CP/MAS) ^{207}Pb NMR spectra of the 1:1 crystalline Pb(II) complex with penicillamine (PbPen), measured at two different spin rates (5.5 and 5.8 kHz) at room temperature (δ_{iso} = 909 ppm, shown by the dashed line; overlapped spectra are shown in Figure S-5a in the Supporting Information).

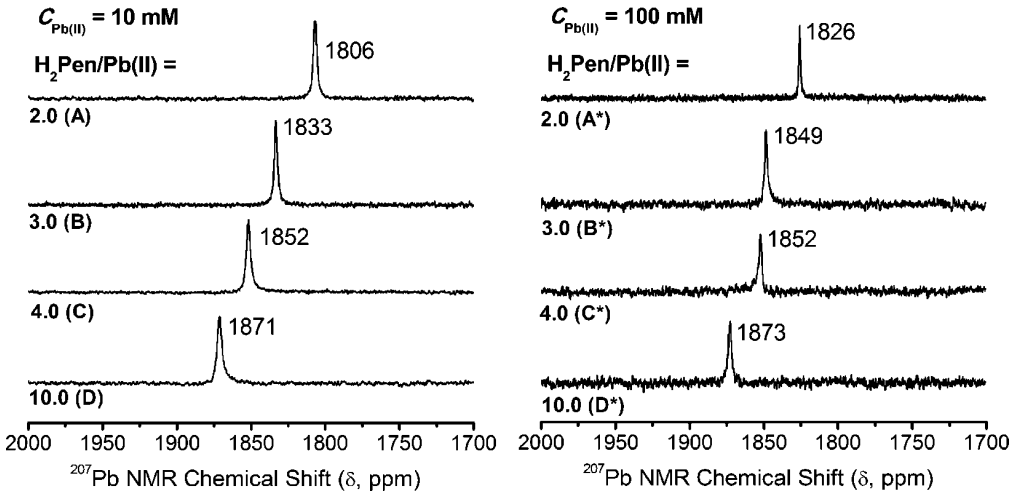

Figure 5. ^{207}Pb NMR spectra of alkaline aqueous solutions (10% v/v D_2O): solutions A–D ($C_{Pb(II)}$ = 10 mM; enriched ^{207}Pb) and solutions A*–D* ($C_{Pb(II)}$ = 100 mM), with H_2Pen/Pb(II) molar ratios of 2.0–10.0.

coordination number increases the shielding on the Pb(II) ion.[46,56]

^{207}Pb NMR spectra for the two sets of alkaline Pb(II)-penicillamine aqueous solutions (10% v/v D_2O) A–D ($C_{Pb(II)}$ = 10 mM; prepared using enriched ^{207}PbO) and A*–D*

dx.doi.org/10.1021/ic5018714 | Inorg. Chem. 2014, 53, 12459–12468

($C_{Pb(II)}$ = 100 mM) containing different H_2Pen/Pb(II) molar ratios, are shown in Figure 5. Solution A* (H_2Pen/Pb(II) = 2.0; pH 11.0) shows a single, sharp signal at 1826 ppm, which could be due to a single, dominating Pb(II)-penicillamine complex, or fast ligand exchange between different Pb(II) species in this solution.

All other spectra in Figure 5 also show a single, relatively narrow peak (width at half height $\Delta\nu_{1/2} \approx$ 100−200 Hz). The broadening is likely due to slower exchange between different Pb(II)-penicillamine species in solution at room temperature on the NMR time scale. For each set of solutions, the NMR peak shows a downfield shift over a narrow $\delta(^{207}Pb)$ range (1806−1871 ppm for solutions A−D; 1826−1873 ppm for solutions A*−D*), as the total ligand concentration increases, suggesting a dominating Pb(II)-penicillamine complex being present. Solutions C and C* with C_{H_2Pen} = 40 and 400 mM, and also solutions D and D* with C_{H_2Pen} = 0.1 and 1.0 M, respectively, show matching ^{207}Pb NMR chemical shifts.

Pb L_{III}-Edge X-ray Absorption Spectroscopy. The X-ray absorption near edge structure (XANES) features, and also the k^3-weighted EXAFS oscillations for the Pb(II)-penicillamine alkaline aqueous solutions A−D ($C_{Pb(II)}$ = 10 mM) and A*−D* ($C_{Pb(II)}$ = 100 mM) overlap closely (see Figures S-6 and S-7 in the Supporting Information), indicating that, despite the large variations in free ligand concentration, there is no obvious change in the Pb(II) speciation. During the least-squares curve-fitting procedure of the k^3-weighted EXAFS spectra, several fitting models were tested (see Table S-3 in the Supporting Information). The fitting results using a $PbS_2(N/O)_2$ model, consisting of two Pb-(N/O) and two Pb−S paths, are summarized in Table 3, with corresponding figures (both in k- and r-space) shown in Figure 6.

Table 3. Least-Squares Curve-Fitting of the k^3-Weighted EXAFS spectra for Pb(II)-Penicillamine Aqueous Solutions A−D ($C_{Pb(II)}$ = 10 mM) and A*−D* ($C_{Pb(II)}$ = 100 mM) (see Figure 6)[a]

		2Pb−(N/O)		2Pb−S	
solution	H_2Pen/Pb(II) molar ratio	R (Å)	σ^2 (Å^2)	R (Å)	σ^2 (Å^2)
A	2.0	2.39	0.021	2.62	0.0058
B	3.0	2.43	0.020	2.64	0.0056
C	4.0	2.45	0.019	2.64	0.0057
D	10.0	2.44	0.020	2.64	0.0057
A*	2.0	2.45	0.021	2.65	0.0051
B*	3.0	2.45	0.017	2.64	0.0050
C*	4.0	2.47	0.018	2.65	0.0058
D*	10.0	2.46	0.019	2.65	0.0058

[a] S_0^2 = 0.9 fixed; k-range = 2.7−12 Å^{-1}; R ± 0.04 Å; σ^2 ± 0.002 Å^2.

For solutions B−D and A*−D*, the average Pb−(N/O) and Pb−S bond distances vary over a narrow range (2.43−2.47 Å and 2.64−2.65 Å, respectively; see Table 3). Solution A has a slightly different phase than solution A* in its EXAFS spectrum (see Figure S-7 in the Supporting Information), corresponding to somewhat shorter mean Pb−(N/O) and Pb−S distances.

DISCUSSION

The Pb(II)-penicillamine alkaline aqueous solutions A−D ($C_{Pb(II)}$ = 10 mM) and A*−D* ($C_{Pb(II)}$ = 100 mM), containing H_2Pen/Pb(II) molar ratios of 2.0−10.0 (Table 1), show closely overlapping XANES and EXAFS spectra (see Figures S-6 and S-7 in the Supporting Information), except for the small phase difference between solutions A and A* (see above). Also, their ^{207}Pb NMR resonance peaks appear between $\delta(^{207}Pb)$ 1806 and 1873 ppm (Figure 5), which is a very narrow range, when compared with the large chemical shift range of ∼17 000 ppm for ^{207}Pb NMR spectroscopy. Therefore, these solutions contain a common dominating Pb(II)-penicillamine complex, even in a large excess of the free ligand.

The fraction diagrams shown in Figures S-1a and S-2a in the Supporting Information represent distributions of Pb(II) species as a function of pH at low $C_{Pb(II)}$ concentration (0.5 mM), where PbPen is soluble. At higher lead(II) concentrations, such as those used in the current study, the solid compound PbPen(c) precipitates; however, to our knowledge, no solubility product has been reported. Based on our observations of the PbPen(c) dissolution and the formation constants reported by Corrie et al. (I = 3.00 M),[30] we could estimate a solubility product of log K_{sp} = −17.4 (log β = 17.4) for PbPen(c), so the diagrams shown in Figure S-1b in the Supporting Information can tentatively represent the chemical compositions of Pb(II)-penicillamine solutions A−D ($C_{Pb(II)}$ = 10 mM) and solutions A* and D* ($C_{Pb(II)}$ = 100 mM) at their corresponding alkaline pH (see Table 1). According to these diagrams, all our solutions are dominated by $[Pb(Pen)_2]^{2-}$, with a minor amount of a hydroxo $[Pb(OH)(Pen)_2]^{3-}$ complex in solutions A and A* (pH = 10.3−11.0), and with some amount of a $[Pb(Pen)(HPen)]^-$ complex in solutions B−D and solution D* (pH 9.6).

When using the most recent formation constants obtained by Crea et al. (I = 0.1 M),[31] the best value estimated for the solubility product for PbPen(c) matching our experimental observations (i.e., the pH at which PbPen(c) dissolved under different ligand concentrations) was log K_{sp} = −16.2. Also according to the diagrams shown in Figure S-2b in the Supporting Information, solutions A and A* are dominated by $[Pb(Pen)_2]^{2-}$, but with a minor amount of another type of hydroxo complex being present, i.e., $[Pb(OH)(Pen)]^-$. The amount of this complex would be small in solutions B and C, and insignificant in solutions D and D* (pH 9.6), with the highest H_2Pen/Pb(II) molar ratio of 10.0.

The charged lead(II) species identified in the gas phase, based on the ESI-MS spectra of solutions A and D in positive mode, have Pb(II):ligand ratios of 1:1 and 1:2, i.e., $[Pb(HPen)]^+$ (m/z = 356.02 amu), $[PbPen + Na^+]^+$ (378.00 amu), $[Pb(HPen)(H_2Pen)]^+$ (505.07 amu) and $[(PbPen)_2 + Na^+]^+$ (733.01 amu); see Figure 1, Figure S-3 in the Supporting Information, and Table 2. The only lead(II) complex observed in ESI-MS negative mode was $[Pb(Pen)(HPen)]^-$ (m/z = 503.05 amu); see Figure S-4 and Table S-1 in the Supporting Information.

The UV-vis spectra of solutions A−D show high absorption in the far-UV region (∼255 nm), with a less intense peak at ca. 298 nm (see Figure 2). The position of the lower-energy band can be compared with those observed for Pb(II) complexes with synthetic cysteine-containing peptides CP-CCCC and CP-CCCH (λ_{max} = 330 nm; PbS_3),[42] glutathione (335 nm; PbS_3),[39] wild-type CadC protein (350 nm; PbS_3) and its Cys → Gly substitution mutants C60G CadC and C7G CadC (325 nm; $PbS_2(N/O)$),[57] for which the coordination environments around the Pb(II) ion were confirmed by X-ray absorption spectroscopy. Moreover, the Pb(II) complex of a synthetic peptide CP-CCHH with two cysteine and two histidine residues shows a blue-shift in its maximum absorption peak,

dx.doi.org/10.1021/ic5018714 | Inorg. Chem. 2014, 53, 12459−12468

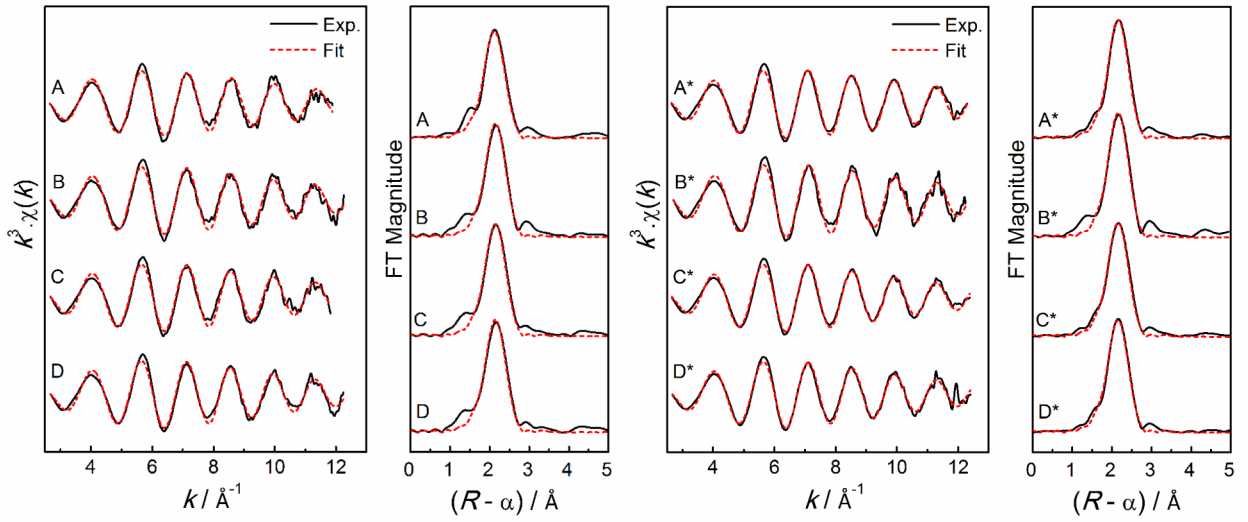

Figure 6. Least-squares curve-fitting of the k^3-weighted Pb L_{III}-edge EXAFS spectra for Pb(II)-penicillamine solutions A–D ($C_{Pb(II)}$ = 10 mM) and A*–D* ($C_{Pb(II)}$ = 100 mM), with H_2Pen/Pb(II) molar ratios of 2.0, 3.0, 4.0, and 10.0, respectively. The corresponding Fourier transforms are also shown. Fitting results are shown in Table 3.

λ_{max} = 310 nm, which has been assigned to PbS_2N_2 coordination.[58] A band at λ_{max} = 295 nm in the UV-vis spectrum of Pb(II):*meso*-DMSA solution has been attributed to a 1:1 chelate with a completely deprotonated ligand ($C_{Pb(II)}$ = 0.02 mM, C_{DMSA} = 2 mM, pH 7.4).[59] PbS_2O coordination was later proposed for such a chelate.[60] The $S^- \rightarrow$ Pb(II) LMCT band for a monothiolate Pb(II) complex $[PbCl(SCH_2CH_2NH_3)](NO_3)$ has been reported at λ_{max} = 260 nm.[61] Furthermore, theoretical calculations of the UV-vis spectra for Pb(II) thiolate complexes suggest that the LMCT band becomes difficult to observe when Pb(II) is surrounded by less that two (cysteine) thiolate groups, because it shows a blue shift and reduced intensity.[62] The above comparison is consistent with a dominating bis-thiolate Pb(II)-penicillamine complex in the Pb(II) penicillamine solutions B–D with overlapping UV-vis spectra (Figure 2), and therefore similar Pb(II) speciation (λ_{max} = 298 nm; $\varepsilon_{max} \approx 4800$ M^{-1} cm^{-1}).

The loss of peak intensity at 298 nm for solution A (Figure 2) could be due to a minor amount of other Pb(II) species with a smaller number of coordinated thiolate groups, such as $[Pb(Pen)(OH)]^-$, as suggested by Crea et al.[31] Considering the high formation constant ($\log \beta_1$ = 13.37–14.32) for the Pb:Pen 1:1 complex,[30,31] solution A does not contain hydrolyzed Pb(II) species (see Figures S-1b and S-2b in the Supporting Information), such as $Pb(OH)_3^-$(aq) ($\log \beta$ = −26.5, I = 1 M $NaClO_4$), for which λ_{max} = 239 nm ($\varepsilon_{max} \approx 2500$ M^{-1} cm^{-1}) has been reported.[63]

The ^{13}C NMR spectra of Pb(II)-penicillamine solutions A and B, which contain the least amount of penicillamine (C_{H_2Pen} = 20 and 30 mM, respectively), showed significant downfield shifts ($\Delta\delta_C$) for the C_1, C_2 and C_3 sites, relative to free penicillamine (see Figure 3 and Table S-2 in the Supporting Information). The largest $\Delta\delta_C$ was observed for the carboxylate C_1 site (6.0–6.5 ppm). Similarly, ^{1}H NMR spectra for solutions A and B showed clear downfield shifts ($\Delta\delta_H$) for H_a (0.34–0.37 ppm) and methyl H_c protons (0.10–0.11 ppm), relative to free penicillamine. The downfield shifts indicate that the penicillamine carboxylate (COO^-), thiolate (S^-), and amine (NH_2) groups are all coordinated to the Pb(II) ions, becoming deshielded.

^{207}Pb NMR spectroscopy can provide specific information about the local structure around Pb(II) ions, considering its sensitivity to the increasing shielding of the ^{207}Pb nucleus by the surrounding donor atoms in the order S < N < O, and the coordination number.[35] The ^{207}Pb NMR peaks observed at $\delta(^{207}Pb) \approx$ 1806–1873 ppm for the alkaline Pb(II)-penicillamine solutions A–D and A*–D* (Figure 5), are downfield relative to that of PbPen (δ_{iso} = 909 ppm) and the reported value for PbS_2O_2 coordination (δ = 1506–1555 ppm),[53] and upfield relative to that of PbS_2N_2 coordination in bis(2-aminoethanethiolato)lead(II) complex (δ_{iso} = 2105), with similar thiolate and amine ligands.[52] Therefore, it is possible to assign the chemical shift of ∼1870 ppm observed for solutions D and D* to a dominating bis-thiolate Pb(II)-penicillamine complex with PbS_2NO coordination, as in the 1:2 complexes $[Pb(S,N,O\text{-Pen})(S\text{-Pen})]^{2-}$ and $[Pb(S,N,O\text{-Pen})(S\text{-HPen})]^-$. The latter complex showed a mass peak at m/z = 503.05 amu (see above). A coordination number higher than four does not seem feasible in this case, because the ^{207}Pb chemical shift would move upfield with increasing coordination number.[64] Moreover, a larger number of shielding O and N atoms surrounding the Pb(II) ion in 5 or 6-coordinated species, such as $[Pb(S,N,O\text{-Pen})(S,O\text{-HPen})]^-$ or $[Pb(S,N,O\text{-Pen})_2]^{2-}$, would be expected to give a ^{207}Pb chemical shift of lower frequency.

Based on the distributions diagrams in Figure S-2b in the Supporting Information, solutions A ($C_{Pb(II)}$ = 10 mM, pH 10.3) and A* ($C_{Pb(II)}$ = 100 mM, pH 11.0), both with a H_2Pen/Pb(II) molar ratio of 2.0, contain a minor amount of the hydroxo complex, $[Pb(Pen)(OH)]^-$, where the −OH group exerts a shielding effect on the ^{207}Pb nucleus. Therefore, the ^{207}Pb chemical shifts of these solutions (δ = 1806–1826 ppm) are somewhat shielded, relative to those of solutions D and D* (∼1870 ppm) for which the amount of the hydroxo complex should be insignificant.

When increasing the molar ratio, and, thus, the free ligand concentration, in both series of solutions (A–D and A*–D*), the ^{207}Pb NMR resonance peak show a downfield shift (Figure 5), which could be due to the $\delta(^{207}Pb)$ sensitivity to the overall change of solution "environment"[35,46,63] (e.g., pH, temperature,

dx.doi.org/10.1021/ic5018714 | Inorg. Chem. 2014, 53, 12459–12468

[Pen^{2-}] and [$HPen^{-}$]), and/or formation of less amount of the hydroxo complex [Pb(Pen)(OH)]$^{-}$. The solution pairs (C, C*) and (D, D*) show similar ^{207}Pb chemical shifts (see Figure 5), indicating that the increasing excess of the ligand has little effect on the chemical composition of their Pb(II) species.

To define the bond distances in the bis-thiolate Pb-(penicillamine)$_2$ complex, Pb L_{III}-edge EXAFS spectroscopy was used. It is noteworthy that the information obtained from ^{207}Pb NMR and EXAFS spectroscopic techniques is complementary, since neighboring ligand atoms in the periodic table (such as N and O) cannot be distinguished by the EXAFS technique,[65] while their ^{207}Pb nuclear shielding is different. The EXAFS spectra of the solutions were measured at room temperature to represent the same speciation, as observed by multinuclear (^{1}H, ^{13}C and ^{207}Pb) NMR spectroscopy.

A comparison of the k^3-weighted Pb L_{III}-edge EXAFS spectra for solid PbPen and solution A* ($C_{Pb(II)}$ = 100 mM; C_{H_2Pen} = 200 mM; pH 11.0), and their corresponding Fourier transforms, clearly shows that the number of coordinated thiolate groups around the Pb(II) ion in solution A* is greater than one (see Figure S-8 in the Supporting Information).

The Pb L_{III}-edge k^3-weighted EXAFS spectra for Pb(II)-penicillamine solutions B–D and A*–D* could be well-fitted with the simulated EXAFS oscillation for a $PbS_2(N/O)_2$ model, yielding mean bond distance values of 2.64 ± 0.04 Å for Pb–S and 2.45 ± 0.04 Å for Pb–(N/O). These distances can be compared with similar average crystallographic distances in four-coordinated Pb(II) complexes: PbS_2N_2 (Pb–S 2.71 Å; Pb–N 2.62 Å) and PbS_2O_2 (Pb–S 2.75 Å; Pb–O 2.40 Å).[39,66] The mean Pb–S distances obtained from the EXAFS refinement of Pb(II)-penicillamine solutions are shorter than the above average crystallographic Pb–S distances. Short Pb–S distances (2.63 Å) have been observed in the crystalline bis(2-aminoethanethiolato)lead(II) complex with PbS_2N_2 coordination.[67] Moreover, the average bond distances obtained from EXAFS data analysis of crystalline PbPen (2 Pb–(N/O) 2.42 ± 0.04 Å and 1 Pb–S 2.68 ± 0.04 Å) were also somewhat shorter than the corresponding distances in its crystal structure: 2.444 and 2.451 Å for Pb–(N/O) and 2.714 Å for Pb–S.[39]

For solution A, somewhat shorter average bond distances were obtained from the EXAFS data analysis (2.62 ± 0.04 Å for Pb–S and 2.39 ± 0.04 Å for Pb–(N/O)) than for the other solutions (see Table 3). As discussed above, also the peak intensity at 298 nm in the UV-vis spectrum was lower, indicating the loss of a thiolate group and the formation of a hydroxo species such as [Pb(Pen)(OH)]$^{-}$, which would be consistent with the shorter average Pb–S and Pb–(N/O) bond distances.

For all Pb(II)-penicillamine solutions, the Debye–Waller factors (DWFs) for the Pb–S path are consistent and reasonable ($\sigma^2 \approx 0.006 \pm 0.001$ Å^2), while corresponding values are quite high for the Pb–(N/O) scattering path (0.019 ± 0.002 Å^2). The DWF for a similar Pb-(N/O) path in crystalline PbPen was also quite high (0.013 ± 0.002 Å^2), even though the Pb–N and Pb–O bond distances in the crystal structure are very similar.[39] Thus, the very high DWF for the Pb–(N/O) path in these Pb(II)-penicillamine solution probably describes a large variation around the average Pb–(N/O) distance. The difficulties associated with separating the Pb–(N/O) scattering contributions in a distorted coordination environment from that of the dominating Pb–S path in the EXAFS oscillation have been extensively discussed previously.[68,69]

We also performed EXAFS least-squares curve-fitting using other models, refining the coordination number for Pb–(N/O) or Pb–S paths (see Table S-3 in the Supporting Information). The residuals ($\mathcal{R}$) were often very similar to that of the $PbS_2(N/O)_2$ model (Model I in Table S-3 in the Supporting Information). For the less-concentrated solutions A–D ($C_{Pb(II)}$ = 10 mM) and also solution B* ($C_{Pb(II)}$ = 100 mM), the Pb–S coordination number often refined to values of <2.0 (except for solution A), whereas for solutions A*, C*, and D* the refined coordination number for the Pb–S path varied between 2.2–2.5 (Model II in Table S-3 in the Supporting Information). Note that the EXAFS spectra of the solution pairs (C, C*) and (D, D*) overlap, as shown in Figure S-7 in the Supporting Information. The reason for this variation in the refined Pb–S contribution could be the noise level of the EXAFS oscillations (see the Experimental Section).

Refinements of the coordination number for the Pb–(N/O) path often resulted in high values (3–5) corresponding to very high values also for the correlated DWF ($\sigma^2 \approx 0.03$ Å^2), which damps the EXAFS contribution of this path at high k-values. Only for solutions A and D*, the refined coordination number for the Pb–(N/O) path attained reasonable values (see Model III in Table S-3 in the Supporting Information). The Pb–(N/O) coordination number was fixed in the final refinements, since a high value for the Pb–(N/O) path will not be in agreement with the observed ^{207}Pb chemical shift (~1800 ppm) for these Pb(II)-penicillamine solutions.

Based on the above experimental results, we propose that, in alkaline aqueous Pb(II)-penicillamine solutions, [Pb(*S,N,O*-Pen)(*S*-H_nPen)]$^{2-n}$ (n = 0–1) complex(es) with PbS_2NO coordination dominate, where one penicillaminate ligand coordinates in tridentate mode, and the other as a monodentate S-donor ligand (see Scheme 3). A [Pb(*S,N*-Pen)(*S,O*-H_nPen)]$^{2-n}$ (n = 0–1) complex with PbS_2NO coordination is unlikely, with the ligands coordinated in two different modes, (S,N) and (S,O). The reason is that, when Pb(II) ions react with *N*-acetylcysteine with only thiol and carboxyl potential donor sites, in 1:2 metal-to-ligand ratio at alkaline pH, the change in the ^{13}C NMR chemical shift of the carboxylate group is only $\Delta\delta_{COO}$ = 0.5 ppm, relative to free *N*-acetylcysteine (compare with $\Delta\delta_{COO}$ = 6.0 ppm for similar Pb(II)-penicillamine solution A), indicating that the carboxylate group of *N*-acetylcysteine is not bound to the Pb(II) ion.[70] Moreover, as the 1:1 Pb(*S,N,O*-Pen) compound crystallizes from alkaline aqueous solution, regardless of the excess of penicillamine,[33] it is very likely that the ligand keeps the same tridentate coordination mode in alkaline solution.

Scheme 3. Proposed Structure for a Pb(II) D-Penicillamine Complex Na[Pb(Pen)(HPen)] Formed in Aqueous Solution at Alkaline pH

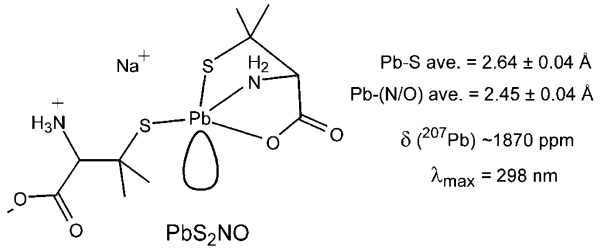

dx.doi.org/10.1021/ic5018714 | Inorg. Chem. 2014, 53, 12459–12468

The mean DWF (0.006 ± 0.001 Å^2) obtained for the Pb−S scattering paths in the [Pb(*S,N,O*-Pen)(*S*-H_nPen)]$^{2-n}$ (n = 0−1) complexes (see Table 3), is relatively small for two Pb−S distances in different coordination modes (*S,N,O*-) and (*S*-) (see Scheme 3), which may be expected to be different in length. For crystalline PbPen(c) (2.714 Å for Pb−S and 3.092 Å for Pb−S′; see Figure S-8 in the Supporting Information), the long Pb−S′ distance evidently makes no contribution to the value obtained by EXAFS for the Pb−S distance (2.68 ± 0.04 Å, DWF = 0.008 ± 0.002 Å). However, the values for the mean Pb−S distances in the Pb(II)-penicillamine solutions are ∼0.04 Å shorter (see Table 3). This is consistent with a shorter (∼0.06−0.07 Å) monodentate Pb−S bond, with higher contribution to the EXAFS oscillation than the Pb−S bond in the tridentate coordination, also because of the inverse relation of EXAFS amplitude to the distance ($1/R^2$).[65] Such a small difference between two similar scattering paths cannot be resolved by EXAFS.

CONCLUSION

So far, the only structural information available on Pb(II) complexes with D-penicillamine, which is a chelating agent against lead toxicity, was the crystal structure comprising the 1:1 complex, Pb(*S,N,O*-Pen).[32,33] The current study shows that penicillamine forms a dominating 2:1 H_2Pen:Pb(II) complex for molar ratios ≥2.0 in aqueous solution when deprotonating the thiol group by increasing the pH (pH = 9.6−11.0). Such Pb(II) species were detected both in positive- and negative-ion mode ESI-MS spectra in the form of [Pb(HPen)(H_2Pen)]$^+$ and [Pb(Pen)(HPen)]$^-$ ions. The combination of the results from ^{1}H NMR, ^{13}C NMR, ^{207}Pb NMR, and UV-vis spectroscopic techniques led us to conclude that a bis-thiolate Pb(II)-penicillamine complex with PbS_2NO coordination is formed, characterized by $\delta(^{207}\text{Pb}) \approx 1870$ ppm and λ_{max} = 298 nm ($\varepsilon_{max} \approx 4800$ M^{-1} cm^{-1}). Its average bond distances are 2.64 ± 0.04 Å for Pb−S and 2.45 ± 0.04 Å for Pb−(N/O), according to the EXAFS data analyses. Under all conditions in this investigaion, including variations in pH and ligand:Pb(II) molar ratio, only the 1:1 PbPen compound with a tridentate *S,N,O*-Pen-ligand could be crystallized from the solutions. Therefore, we propose that the structure of the bis-thiolate Pb(II)-penicillamine complex in solution is [Pb(*S,N,O*-Pen)(*S*-H_nPen)]$^{2-n}$ (n = 0−1), where one penicillamine is bound to the Pb(II) ion in a tridentate (*S,N,O*-) mode, and the other acts as a monodentate (-S) ligand (recall Scheme 3). Such a coordination environment, e.g., Pb(*S,N,O*-Pen)(*S*-cysteine), may explain how penicillamine acts *in vivo*, and inspire rational design of future chelating agents to be used as antidotes against lead toxicity.

ASSOCIATED CONTENT

Supporting Information

Fraction diagrams showing distribution of Pb(II) species based on formation constants reported for Pb(II)-penicillamine complexes; ESI-MS spectra of solutions A (negative (−) ion mode) and D (negative (−) and positive (+) ion mode) and assignment of mass ions; CP/MAS ^{207}Pb NMR spectra of crystalline PbPen measured at two different spin rates, and the static powder pattern reconstructed to obtain the principal components; comparison between Pb L_{III}-edge XANES spectra for solutions (A, D) and (A*, D*), as well as EXAFS spectra for the two sets ($C_{Pb(II)}$ = 10 mM and 100 mM), together with their least-squares curve-fitting results using different models; comparison between EXAFS oscillations and corresponding Fourier transforms for solid PbPen and solution A*. This material is available free of charge via the Internet at http://pubs.acs.org.

AUTHOR INFORMATION

Corresponding Author

*E-mail: faridehj@ucalgary.ca.

Notes

The authors declare no competing financial interest.

ACKNOWLEDGMENTS

We express our sincere gratitude to Dr. Michelle Forgeron, Jian Jun (Johnson) Li, and Dorothy Fox at the instrumentation facility at the Department of Chemistry, University of Calgary, for their assistance with NMR measurements, and to Mr. Wade White for measuring the ESI-MS spectra. CP/MAS solid-state ^{207}Pb NMR of PbPen was measured by Dr. Glenn A. Facey at the Department of Chemistry, University of Ottawa. Beam time was allocated and XAS measurements were carried out at the Stanford Synchrotron Radiation Lightsource (SSRL; Proposal No. 2848 and 3637). Use of the SSRL, SLAC National Accelerator Laboratory, is supported by the U.S. Department of Energy, Office of Science, Office of Basic Energy Sciences under Contract No. DE-AC02-76SF00515. The SSRL Structural Molecular Biology Program is supported by the DOE Office of Biological and Environmental Research, and by the National Institutes of Health, National Institute of General Medical Sciences (including P41GM103393). The contents of this publication are solely the responsibility of the authors and do not necessarily represent the official views of NIGMS or NIH. We are grateful to the National Science and Engineering Research Council of Canada (NSERC), Canadian Foundation for Innovation (CFI), the Province of Alberta (Department of Innovation and Science) and the University of Calgary for their financial support.

REFERENCES

(1) Winter, M.; Brodd, R. J. *Chem. Rev.* **2004**, *104*, 4245−4270.
(2) Patil, A.; Bhagwat, V.; Patil, J.; Dongre, N.; Ambekar, J.; Jailkhani, R.; Das, K. *Int. J. Environ. Res. Public Health* **2006**, *3*, 329−337.
(3) Patrick, L. *Altern. Med. Rev.* **2006**, *11*, 2−22.
(4) Baltrusaitis, J.; Chen, H.; Rubasinghege, G.; Grassian, V. H. *Environ. Sci. Technol.* **2012**, *46*, 12806−12813.
(5) Villa, J. E. L.; Peixoto, R. R. A.; Cadore, S. *J. Agr. Food Chem.* **2014**, *62*, 8759−8763.
(6) Farfel, M.; Chisolm, J. *Environ. Res.* **1991**, *55*, 199−212.
(7) Godwin, H. *Curr. Opin. Chem. Biol.* **2001**, *5*, 223−227.
(8) Palaniappan, P. R.; Krishnakumar, N.; Vadivelu, M. *Environ. Chem. Lett.* **2009**, *7*, 51−54.
(9) Gidlow, D. A. *Occup. Med.* **2004**, *54*, 76−81.
(10) Lowry, J. A. *Oral Chelation Therapy for Patients with Lead Poisoning*; World Health Organization: Geneva, Switzerland, 2010; pp 1−13.
(11) Needleman, H. *Annu. Rev. Med.* **2004**, *55*, 209−222.
(12) Bressler, J.; Kim, K.-A.; Chakraborti, T.; Goldstein, G. *Neurochem. Res.* **1999**, *24*, 595−600.
(13) Erskine, P.; Senior, N.; Awan, S.; Lambert, R.; Lewis, G.; Tickle, I.; Sarwar, M.; Spencer, P.; Thomas, P.; Warren, M.; Shoolingin-Jordan, P.; Wood, S.; Cooper, J. *Nat. Struct. Biol.* **1997**, *4*, 1025−1031.
(14) Bridgewater, B.; Parkin, G. *J. Am. Chem. Soc.* **2000**, *122*, 27140−7141.
(15) Simons, T. J. *Eur. J. Biochem.* **1995**, *234*, 178−183.
(16) Beattie, A. D. *Proc. R. Soc. Med.* **1977**, *70*, 43−45.
(17) Chisolm, J. *J. Pediatr.* **1968**, *73*, 1−38.

(18) Goldberg, A.; Smith, J.; Lochhead, A. *Br. Med. J.* **1963**, 1270−1275.
(19) Shannon, M.; Graef, J.; Lovejoy, F. *J. Pediatr.* **1988**, *112*, 799−804.
(20) Andersen, O. *Chem. Rev.* **1999**, *99*, 2683−2710.
(21) Stefania, M.; Diana, S.; Caruso, A.; Saturnino, C. *Arch. Toxicol.* **2010**, *84*, 501−520.
(22) Volans, G. N.; Karalliedde, L.; Wiseman, H. M. *Review of Succimer for Treatment of Lead Poisoning*; World Health Organization: Geneva, Switzerland, 2010.
(23) Gourlaouen, C.; Parisel, O. *Int. J. Quantum Chem.* **2008**, *108*, 1888−1897.
(24) Goyer, R. A.; Cherian, M. G.; Jones, M. M.; Reigart, J. R. *Environ. Health Perspect.* **1995**, *103*, 1048−52.
(25) Shannon, M.; Townsend, M. *Ann. Pharmacother.* **2000**, *34*, 15−18.
(26) Blanusa, M.; Varnai, V. M.; Piasek, M.; Kostial, K. *Curr. Med. Chem.* **2005**, *12*, 2771−94.
(27) Avdeef, A.; Kearney, D. L. *J. Am. Chem. Soc.* **1982**, *104*, 7212−7218.
(28) Kuchinskas, E. J.; Rosen, Y. *Arch. Biochem. Biophys.* **1962**, *97*, 370−372.
(29) Lenz, G. R.; Martell, A. E. *Biochemistry* **1964**, *3*, 745−750.
(30) Corrie, A. M.; Walker, M. D.; Williams, D. R. *J. Chem. Soc., Dalton Trans.* **1976**, 1012−1015.
(31) Crea, F.; Falcone, G.; Foti, C.; Giuffre, O.; Materazzi, S. *New J. Chem.* **2014**, *38*, 3973−3983.
(32) Freeman, H.; Stevens, G.; Taylor, I. *J. Chem. Soc. Chem. Comm.* **1974**, 366−367.
(33) Schell, A.; Parvez, M.; Jalilehvand, F. *Acta Crystallogr., Sect. E: Struct. Rep. Online* **2012**, *E68*, m489−m490.
(34) Glasoe, P. K.; Long, F. A. *J. Phys. Chem.* **1960**, *64*, 188−190.
(35) Wrackmeyer, B.; Horchler, K.; Webb, G. A. ^{207}Pb-NMR Parameters. In *Annual Reports on NMR Spectroscopy*, Vol. *22*; Webb, G. A., Ed.; Academic Press: San Diego, CA, 1990; pp 249−306.
(36) van Gorkom, L. C. M.; Hook, J. M.; Logan, M. B.; Hanna, J. V.; Wasylishen, R. E. *Magn. Reson. Chem.* **1995**, *33*, 791−795.
(37) Willans, M. J.; Demko, B. A.; Wasylishen, R. E. *Phys. Chem. Chem. Phys.* **2006**, *8*, 2733−2743.
(38) Ressler, T. *J. Synchrotron Rad.* **1998**, *5*, 118−122.
(39) Mah, V.; Jalilehvand, F. *Inorg. Chem.* **2012**, *51*, 6285−6298.
(40) Ankudinov, A. L.; Rehr, J. J. *Phys. Rev. B* **1997**, *56*, R1712−R1716.
(41) Zabinsky, S. I.; Rehr, J. J.; Ankudinov, A.; Albers, R. C.; Eller, M. J. *Phys. Rev. B* **1995**, *52*, 2995−3009.
(42) Magyar, J.; Weng, T.-C.; Stern, C.; Dye, D.; Payne, J.; Bridgewater, B.; Mijovilovich, A.; Parkin, G.; Zaleski, J.; Penner-Hahn, J.; Godwin, H. *J. Am. Chem. Soc.* **2005**, *127*, 9495−9505.
(43) Wang, Y.; Hemmingsen, L.; Giedroc, D. *Biochemistry* **2005**, *44*, 8976−8988.
(44) Ghering, A.; Miller Jenkins, L.; Schenck, B.; Deo, S.; Mayer, A.; Pikaart, M.; Omichinski, J.; Godwin, H. *J. Am. Chem. Soc.* **2005**, *127*, 3751−3759.
(45) Vogler, A.; Nikol, H. *Pure Appl. Chem.* **1992**, *64*, 1311−1317.
(46) Harrison, P. G.; Healy, M. A.; Steel, A. T. *J. Chem. Soc., Dalton Trans.* **1983**, 1845−1848.
(47) Dmitrenko, O.; Bai, S.; Beckmann, P.; Bramer, S.; Vega, A.; Dybowski, C. *J. Phys. Chem. A* **2008**, *112*, 3046−3052.
(48) Van Bramer, S. E.; Glatfelter, A.; Bai, S.; Dybowski, C.; Neue, G.; Perry, D. L. *Magn. Reson. Chem.* **2006**, *44*, 357−365.
(49) Fayon, F.; Farnan, I.; Bessada, C.; Coutures, J.; Massiot, D.; Coutures, J. P. *J. Am. Chem. Soc.* **1997**, *119*, 6837−6843.
(50) Andersen, R. J.; diTargiani, R. C.; Hancock, R. D.; Stern, C. L.; Goldberg, D. P.; Godwin, H. A. *Inorg. Chem.* **2006**, *45*, 6574−6576.
(51) Briand, G.; Smith, A.; Schatte, G.; Rossini, A.; Schurko, R. *Inorg. Chem.* **2007**, *46*, 8625−8637.
(52) Jalilehvand, F.; Sisombath, N.; Schell, A. C.; Facey, G. A. *Inorg. Chem.* Submitted for publication.
(53) Rupprecht, S.; Franklin, S. J.; Raymond, K. N. *Inorg. Chim. Acta* **1995**, *235*, 185−194.
(54) Neupane, K. P.; Pecoraro, V. L. *Angew. Chem., Int. Ed.* **2010**, *49*, 8177−8180.
(55) Burnett, T. R.; Dean, P. A. W.; Vittal, J. J. *Can. J. Chem.* **1994**, *72*, 1127−1136.
(56) Kennedy, J. D.; McFarlane, W.; Pyne, G. S. *J. Chem. Soc., Dalton Trans.* **1977**, 2332−2336.
(57) Busenlehner, L.; Weng, T.-C.; Penner-Hahn, J.; Giedroc, D. *J. Mol. Biol.* **2002**, *319*, 685−701.
(58) Payne, J.; Horst, M.; Godwin, H. *J. Am. Chem. Soc.* **1999**, *121*, 6850−6855.
(59) Harris, W. R.; Chen, Y.; Stenback, J.; Shah, B. *J. Coord. Chem.* **1991**, *23*, 173−186.
(60) Fang, X.; Fernando, Q. *Chem. Res. Toxicol.* **1995**, *8*, 525−536.
(61) Bharara, M. S.; Parkin, S.; Atwood, D. A. *Inorg. Chim. Acta* **2006**, *359*, 3375−3378.
(62) Jarzęcki, A. A. *Inorg. Chem.* **2007**, *46*, 7509−7521.
(63) Perera, W. N.; Hefter, G.; Sipos, P. M. *Inorg. Chem.* **2001**, *40*, 3974−3978.
(64) Margolis, L. A.; Schaeffer, C. D.; Yoder, C. H. *Appl. Organomet. Chem.* **2003**, *17*, 236−238.
(65) Penner-Hahn, J. E. X-ray Absorption Spectroscopy. In *Comprehensive Coordination Chemistry II, Vol. 2*; McCleverty, J. A., Meyer, T. J., Eds.; Pergamon Press: Oxford, U.K., 2003; Chapter 13; pp 159−186.
(66) Allen, F. H. *Acta Crystallogr., Sect. B: Struct. Sci.* **2002**, *B58*, 380−388.
(67) Fleischer, H.; Schollmeyer, D. *Inorg. Chem.* **2004**, *43*, 5529−5536.
(68) Manceau, A.; Boisset, M.-C.; Sarret, G.; Hazemann, J.-L.; Mench, M.; Cambier, P.; Prost, R. *Environ. Sci. Technol.* **1996**, *30*, 1540−1552.
(69) Bargar, J. R.; Brown, G. E., Jr; Parks, G. A. *Geochim. Cosmochim. Acta* **1997**, *61*, 2617−2637.
(70) Sisombath, N.; Jalilehvand, F. Manuscript in preparation.